

SOME EXPERIENCES FROM THE COMMISSIONING PROGRAM OF THE SLC ARCS*

G. E. FISCHER, K. L. BROWN, F. BULOS, T. FIEGUTH, A. HUTTON,
J. J. MURRAY, N. TOGE, W. T. WENG, H. WIEDEMANN†

Stanford Linear Accelerator Center
Stanford University, Stanford, California 94305

1. Abstract

The SLC Arc System is designed to transport beams of electrons and positrons from the end of the SLAC Linac to the beginning of the Final Focus System where they are made to collide head on. To minimize phase space dilution caused by quantum processes in the synchrotron radiation energy loss mechanism, the bending radii are large (279 m) and very high gradient ($n = 32824$) AG cells are arranged in trains of low dispersion, terrain following achromats. First experiences in operating a system of over 900 magnets, each with beam position monitors and corrector magnet movers, spanning 9000 feet, are described.

2. Introduction

The beam optical design of the SLC Arc Transport System has been described,¹ and treated most recently by Fieguth *et al.*,² at this conference. Before commenting on the performance of the system we will briefly review its salient design features and the properties of the components.

Layout:

Electrons and positrons are transported from the end of the SLAC linac to the beginnings of the Final Focus System in a site dominated geometry shown in Fig. 1.

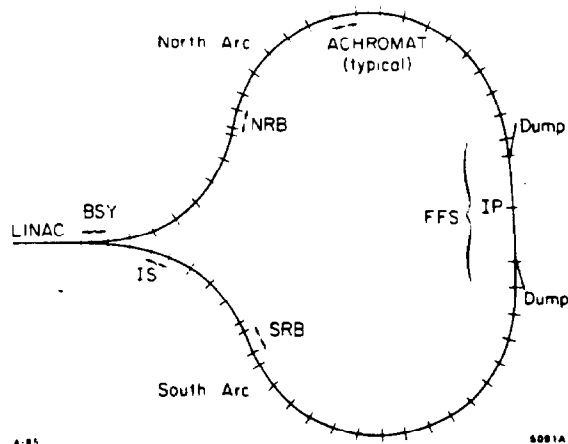


Fig. 1. SLC ARC Layout, typical sections are achromats

Special matching sections are introduced: 1) In the Beam Switchyard (BSY) to separate, momentum analyse and launch the beams into the arcs with the appropriate position, angle and dispersion function. 2) Reverse Bend sections (NRB, SRB) to invert the dispersion function in regions of curvature inflection. 3) An Instrument Section (IS) to accommodate the geometry of the south arc. The SLC arc tunnels are not in a plane, but are, as shown in Fig. 2, arranged to follow the geologic contours of the terrain and to avoid, among other things, the PEP tunnels.

Lattice:

The main arcs are comprised of very strong focussing AG FODO cells having a phase shift per cell of 108° in each plane.

*Work supported by the Department of Energy, contract DE-AC03-76SF00515.
† SSRL - Stanford University.

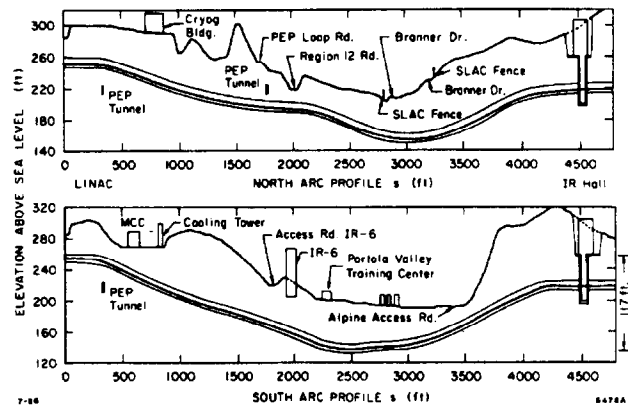


Fig. 2 Vertical profiles of the SLC Arcs.

Generally 10 cells, (*i.e.*, 20 magnets) are arranged to form a second order achromat with a phase shift of 6π . Each arc contains 23 achromats, interrupted by special sections, each of which has a unity transfer matrix, in order to preserve the achromatic character of the overall system. The β and η functions of one cell are shown in Fig. 3. Note that the average eta function has been suppressed to 35 mm in order to combat emittance growth caused by fluctuations in the synchrotron radiation loss mechanism. Whole achromats are rolled about the beam axis to provide the required terrain following vertical deflections.

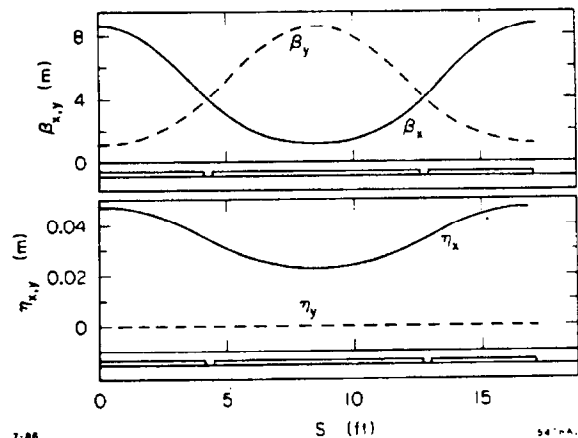


Fig. 3 Lattice functions of an Arc AG cell.

3. System Description

AG Magnets:

The design and construction of these magnets has been described.³ A cross section of the magnet is shown in Fig. 4. At 50 Gev, the dipole guide field is 6 KG, the gradient 7 KG/cm, with a superimposed sextupole of 1.6 and -2.7 KG/cm² in the F and D magnets, respectively. 2.5 m long, they have no coils *per se*, but are series excited by means of aluminum bus bars that are joined every four units. Installation was completed last July.

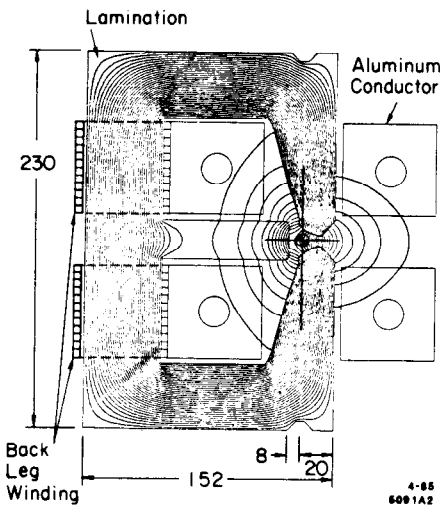


Fig. 4. Schematic cross section of SLC AG Magnets (in mm).

Photo 1 shows a portion of the south arc tunnel with alignment in progress. Backleg windings are provided to adjust the magnetic fields (for the energy loss along the arcs caused by synchrotron radiation) on an achromat by achromat basis. The total loss, varying as E^3 , amounts to $\approx 2.4\%$ at 50 Gev.



Photo 1. View of a portion of the South Arc Tunnel Survey and Alignment:

The methods employed have been described previously⁴ and at this conference.⁵ A surface net was established with both modern conventional techniques and by means of navigational satellites (GPS). The closing error of this net was about 2 mm. This net was transferred below ground and an intersecting laser beam method was used to locate the design orbit at each pedestal. Magnets were installed, resurveyed and finally aligned relative to each other taking into account their mechanical and magnetic imperfections. Tolerances recommended by the Beam Dynamics Task Force⁶ are listed in Table I below.

Table I

Transverse alignment (magnets and quads)	100 μm rms
Axial position error (magnets and quads)	1000 μm rms
Roll (magnets and quadrupoles)	1 milliradian rms
Field excitation ΔB	1 part per 10^3 rms
Displacement of Beam Position Monitors	100 μm rms
Reproducibility of MM corrector position	15 μm rms

Figure 5 shows the results of the last magnet-to-magnet alignment in the tunnel before the final smoothing adjustments were applied, indicating that the requested tolerances will indeed be achieved.

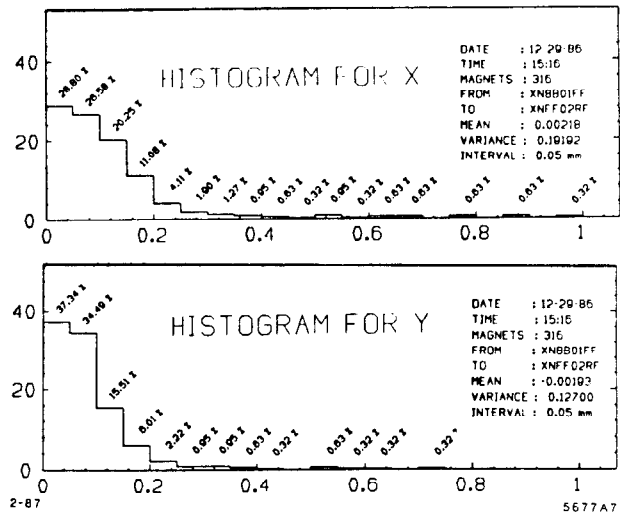
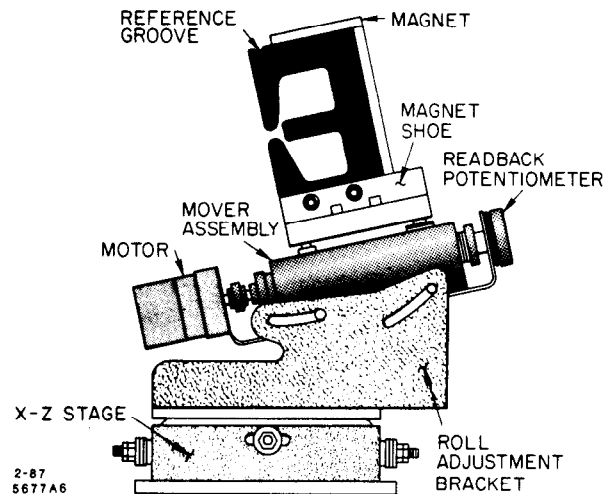


Fig. 5. Distribution of residual alignment errors(see Text)

Orbit Correction:

Even if the above listed alignment tolerances are met, since the gradients superimposed on the guide field are extreme, an on-line orbit correction system is required to keep the centroid of the beam to within about a millimeter of the design orbit. This ensures that the optics remain linear, β and η beats remain tolerable and little additional phase space dilution takes place. For this machine, were it confined to bend in a plane, such a magnet moving scheme would be completely nondispersive.⁷

We have chosen to equip the upstream end of each AG magnet with a motor driven actuator as illustrated in Fig. 6. Horizontally focussing magnets are moved in the local horizontal coordinate, defocussing in the vertical. Attached to the moving end of each magnet is a beam position monitor⁸ (BPM) which is summed to read Δx on an F and Δy on a D magnet. The phase shift of the transfer coefficient (the angle introduced by the magnet motion to the beam deflection seen at the nearest like sign BPM) is nearly 90° .



This "one on one" steering method, which is applied sequentially down the arc, has been automated using the SLC control computer. The algorithms employed take into account mechanical backlash of the movers, providing, thereby, a setting resolution of about $10 \mu\text{m}$. The estimated resolution of reading the BPM's, averaged over say 10 pulses, is $50 \mu\text{m}$. Each BPM has had its electrical center measured in the laboratory and its physical position, relative to the magnetic center of the magnet, taken into account. At present, it takes about 15 minutes to "steer" through each achromat. This time will be shortened when algorithms, that apply an N by N correction, are commissioned.

Other Diagnostic Instrumentation:

Since at full design current and repetition rate each beam carries 70 KW, the arcs are provided with toroid beam current monitors that are wired into a Machine Protection System that can turn off either or both beams on a pulse by pulse basis. All collimators are provided with heat sensors and ion chambers. Insertable zinc-sulphide screens (inherent resolution $\approx 50 \mu\text{m}$) are available to measure energy width and beam sizes at several locations. A set of momentum defining slits in the BSY region serve to permit passage of beams into the arcs of only the correct energy.

4. Performance to Date

Figure 7 shows that we have successfully transmitted an electron beam of 47 GeV through to the end of the north arc. The bottom trace is proportional to the sum signal from the BPMs and shows $\approx 100\%$ transmission. The upper traces show the magnitudes of residual orbit errors in x and y after the steering program was implemented in a preliminary way.

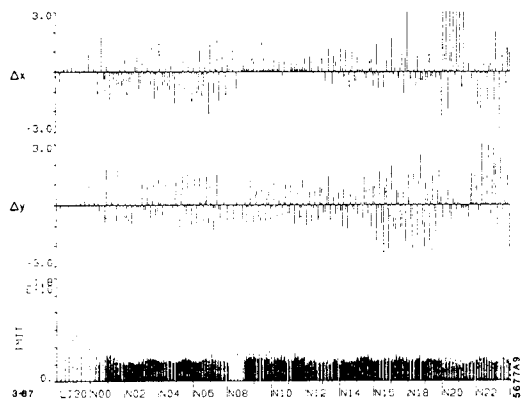


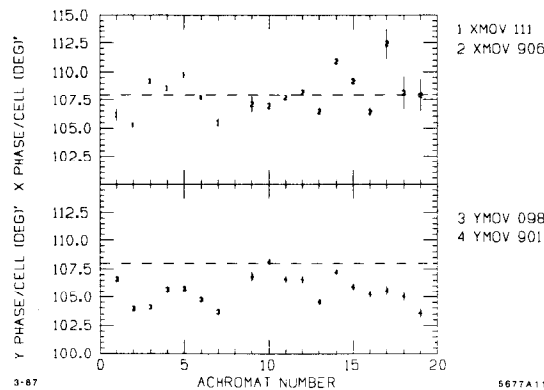
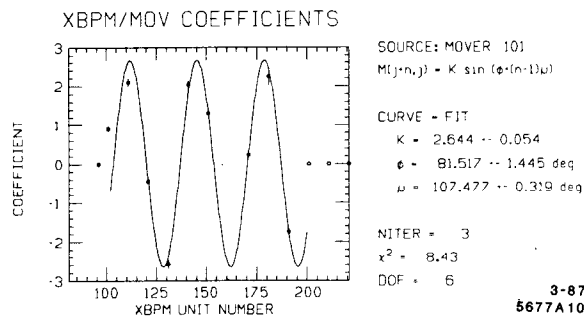
Fig. 7. Orbit and transmission through North Arc

Figure 8 is a television camera photo of the beam at a profile monitor located in the NRB region. The black spot is a hole in the screen which is $300 \mu\text{m}$ in diameter. A digitization of the beam spot projected on the horizontal axis shows the beam to have $\sigma_x = 139 \mu\text{m}$, quite close to the design value of $120 \mu\text{m}$.

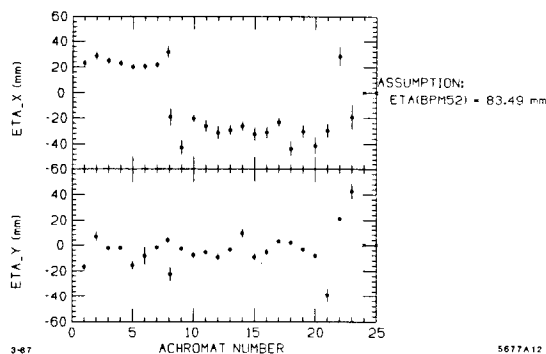


Fig. 8. Beam Size in NRB section, $\beta_x = \beta_y = 40 \text{ m}$

Figure 9 shows the orbit of a deliberately induced betatron oscillation. The BPM data is fitted to display the phase shift per cell and MM to BPM transfer coefficient. The phase shifts for each achromat are displayed in Fig. 10 showing relatively little disagreement with theory.



Figs. 9 and 10 (see text). Values for η_x and η_y were determined by changing the incident beam energy. Preliminary data for North Arc η values are shown below in Fig. 11.



5. Conclusions

Although a great many experiments remain to be done to check the details of the optical design and overall system performance, our initial experiences, obtained with a rather limited amount of beam time, show that the north arc is suitable for colliding beam trials.

Acknowledgments

We wish to express our sincerest thanks to the many engineers, designers and technicians who contributed to the building of this project over the last three years. We wish also to thank the installation and checkout teams and the operations staff without whose dedicated efforts these results would not have been achieved.

References

1. S. Kheifets *et al.*, 13th Int. Conf. High Energy Acc., Novosibirsk, USSR, Aug 1986; SLAC-PUB-4013.
2. T. Fieguth *et al.*, these Proceedings.
3. G. E. Fischer *et al.*, IEEE Trans. Nuc. Sci. NS-32, 3657 (1985).
4. H. Friedsam *et al.*, ASP-ACSM Meeting, Washington (1985).
5. R. Pitthan *et al.*, these Proceedings.
6. Studies carried out from 1982 to present by K. Brown, A. Chao, T. Fieguth, J. Jaeger, S. Kheifets, J. Murray, R. Servranckx, H. Shoaee; see also Weng *et al.*, this conference.
7. J. J. Murray *et al.*, SLC-CN-338 (1986) and W. Weng, M. Sands SLC-CN-339 (1986).
8. J. L. Pelegrin, M. Ross, B. Scott, these Proceedings.